Journal of Materials Chemistry A

Accepted Manuscript

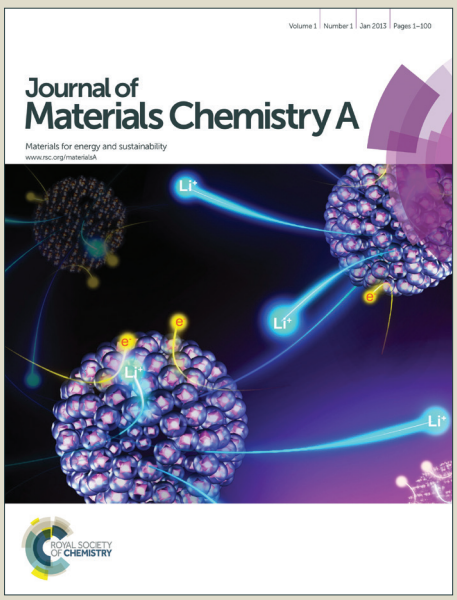

ROYAL SOCIETY OF CHEMISTRY

www.rsc.org/materialsA

Journal Name

ARTICLE

A Triazine-Resorcinol based Porous Polymer With Polar Pores and Exceptional Surface Hydrophobicity Showing CO_2 Uptake Under Humid Conditions

Received 00th January 20xx,
Accepted 00th January 20xx

DOI: 10.1039/x0xx00000x

www.rsc.org/

Shyamapada Nandi,[a] Ulrike Werner-Zwanziger,[b] and Ramanathan Vaidhyanathan.[a†]

ABSTRACT. Several applications including post-combustion carbon capture require capturing CO_2 under humid conditions. To obtain a material capable of interacting stronger with CO_2 than water, surface hydrophobicity and polarizing pores have been incorporated simultaneously into an ultra-microporous Bakelite-type polymer comprising of triazine-triresorcinol building units. Being built from C-C bonds, it exhibits exceptional chemical stability (survives conc.HNO_3(g) + SO_3(g) without losing any porosity). Triazine-Phenol lined channels enables adsorption of CO_2 (2.8 mmol g^{-1} with good selectivity of 120:1 (85%N_2:15%CO_2) at 303K, 1bar) and the inherent surface hydrophobicity amply minimizes the affinity for H_2O. When the adsorption was carried out using a humid CO_2 stream (~50% RH) the material loses only about 5% of its capacity. In a steam-conditioning experiment, the sample was exposed to high humidity (~75% RH) for a day, and without any further activation, was tested for CO_2 adsorption. It retains more than 85% of its CO_2 capacity. And this capacity was intact even after 48hrs of steam conditioning. The role of phenol in contributing to the surface hydrophobicity is exemplified by the fact that a ~17% lithiation of the phenolic sites nearly removes all of the surface hydrophobicity. The local structure of the polymer has been modeled using Tight Binding DFT methods (Accelrys) and three low energy conformers were identified. Only the CO_2 isotherm simulated using the lowest energy conformer matches the experimental isotherm quite well. The triazine-phenol polymer presented here has good hydrophilic-hydrophobic balance, where the basic triazine units and the phenol groups seems to co-operatively assist the CO_2 capture under humid conditions. These properties along with its excellent acid stability makes the material a suitable candidate for post-combustion CO_2 capture. Also, the study presents a new approach to simultaneously introducing polarizing character and surface hydrophobicity into a porous material.

Introduction

High surface area Metal Organic Frameworks (MOFs), Covalent Organic Frameworks (COFs), porous polymers, traditional zeolites and inorganic mesoporous materials are being investigated steadily for their applications in gas capture and separation.[1-10] In many of the metal-organic based sorbents there are still severe concerns regarding their stability to extremely harsh environments which constitute majority of the industrial effluents (steam, acidic vapors, basic conditions and particulates etc).[1-4,11-14] To address water stability, recently, modification in terms of choice of metal (Zr, Al, Cr, Ni) or hydrophobic side chains or protecting groups on the ligand backbone have been carried out to improve the stability.[15-19] Here we have taken a slightly different approach, wherein we have made metal-free organic frameworks built from exceptionally strong C-C bond to address the stability issues. Of course, similar approach has been adopted before, resulting in several porous polymers and composites.[6,20-34] Some of them have shown excellent stabilities and CO_2 capture capabilities.[27-34] Recently, a family of porous covalent triazine frameworks (PCTF)[35] have been made under ionothermal conditions. They have nano to microporous frameworks and some show exceptionally high surface areas (2235 m^2/g)[36] and exhibit good selectivities for CO_2 over N_2 and CH_4.[35,36] Melamine based microporous organic polymers,[37] polymer nanosieve membranes,[38] polyethylene type porous organic polymer have also been investigated for gas adsorptions.[39] However, very few polymers have a CO_2 uptake above 2 mmol g^{-1} under ambient conditions (Table S1) with reasonable selectivity (>100). For example, some of the Porous Aromatic Framework (PAF) series show uptakes in excess of 2 mmol g^{-1} under ambient conditions.[40] A series of porous polymer networks (PPNs) with exceptionally high surface areas and high pressure CO_2, CH_4 and H_2 capacities have been reported by Yuan et al.[31] But the compounds from both the PAF and PPN series do not have sufficiently high CO_2 selectivities. However, loading of polyamines into PAF-5 gave excellent CO_2 adsorbents, but such sorbents requiring a guest loading could have issues with obtaining consistent guest

[a] Department of Chemistry, Indian Institute of Science Education and Research, Dr. Homi Bhabha Road, Pashan, Pune-411008, Maharashtra-India. E-mail: vaidhya@iiserpune.ac.in.
[b] Department of Chemistry, IRM, NMR-3, Dalhousie University, 6274 Coburg Road , PO BOX 15000, Halifax, NS B3H4R2 , Canada.
† corrospondance to vaidhya@iiserpune.ac.in
Electronic Supplementary Information (ESI) available from www.rsc.org.
See DOI: 10.1039/x0xx00000x

loading across multiple batches and during scale up, which has been realized also by the authors.[41] We believe it is advantageous to have the active sites as a part of the framework. The advantage of using porous organic polymers was exemplified in a recent report wherein humidity swing was employed to carry out CO_2 capture.[42] Also, the inherent ability of polymer derived porous carbons to capture CO_2 under humid conditions was demonstrated by Lu and co-workers.[43] In addition to the consideration of the stability of the material to humidity, its impact on CO_2/N_2 separation is also important.[9,27,44]

In a typical post-combustion CO_2 capture by solid adsorbent the effluent or flue gas at 90-100ºC is cooled down to 50-30ºC, stripped of acidic vapors (NOx, SOx) and water vapors and then the relatively dry stream (85%N_2:15%CO_2) is fed to the CO_2 recovery/adsorption unit.[3,11,45] The extent to which the flue gas stream is stripped of acidic fumes and dried has a direct impact on the cost and design complexity involved in the capture process itself. Developing solid sorbents which exhibits very good stability towards heat, steam and acidic fumes, with good CO_2 uptake at room temperature and 1 bar and high CO_2/N_2 selectivity could minimize or take away stripping of humidity and reactive vapors and thereby could bring down the parasitic load on the process. Cross-linked organic oligomers and polymers are known for their exceptional chemical and thermal stability.[24-31,46,47] When made from bulky monomers devoid of highly polar acidic or basic functionalities these cross-linked polymers occur as insoluble powder, however, they generally do not have sufficient functionality to polarize gas molecules or to interact with them via other weak forces. Many of them show N_2 uptake at 77K while their CO_2 capture abilities have not been explained.[24,25,39] In the microporous polymers wherein CO_2 capture has been observed,[25,48] majority of the CO_2 capture happens via gas trapping in the micropores, and such pores could be amenable to water molecules as well. Very recently, CO_2 capture using benzimidazole and triazine based polymers were reported,[49,50] but they were not evaluated for CO_2 capture under humid conditions. To capture CO_2 under the humid flue gas conditions, functionalizing a pore with polarizing and basic groups favoring interactions with CO_2 and simultaneously providing hydrophobicity to the pores would be effective, but this is quite challenging. In fact, MOFs made of highly polar carboxylates, phosphonates, sulfonates tend to interact with CO_2 via dispersive, electrostatic and quadrupolar forces which make them as excellent CO_2 sorbents.[51] Similarly, zeolites used in CO_2 scrubbing, Zeolite-13x, has polarizing pore walls.[52,53] Unfortunately, most of these polar MOFs, adhere water as much as they do CO_2. When such polar groups are sheathed by protective groups, a drastic decrease in CO_2-framework interactions results,[54] this makes tuning the material for CO_2 over water a very tricky task. In an attempt to address the stability issues and capture of CO_2 under humid conditions, here, we report a triazine-triresorcinol based ultra-microporous polymer having highly hydrophobic surface and polar pore walls combining to form a Hydrophobic Polar Framework (HPF-1). Furthermore, we have used Tight Binding Density Functional Theory (DFT-TB) calculations to simulate the structure of HPF-1, something which is being employed increasingly in the recent times to obtain meaningful structural insights on amorphous polymers.[55,56]

Experimental

The polymer is prepared using simple Bakelite chemistry by reacting triazine-triresorcinol with terephthaldehyde under solvothermal conditions. A reaction between 4,4',4''-(1,3,5-triazine-2,4,6-triyl)tris(benzene-1,3-diol) (0.203g; 0.5mmol) and terephthaldehyde (0.100g; 0.75mmol) in a solution containing 5ml 1,4-dioxane + 3ml tetrahydrofuran was carried out by heating at 200ºC for 96hrs (Figure 1). The product, yellowish brown color powder was isolated by filtration and was washed with dimethylformamide (15ml), tetrahydrofuran (10ml) and finally with methanol and acetone. The powder was found to be amorphous from powder X-ray diffraction (Figure S1).

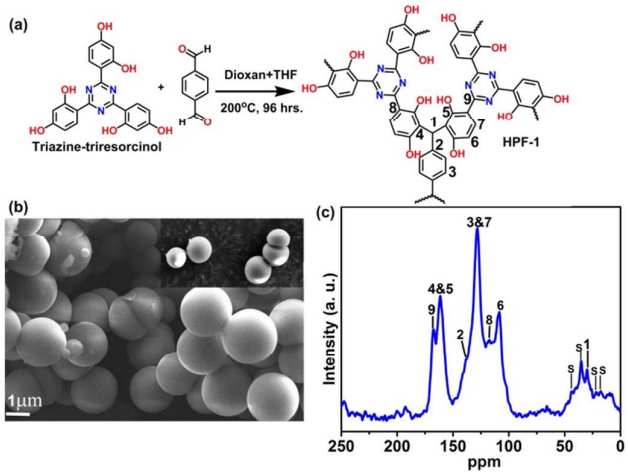

Figure 1. (a) Figure shows the reaction involved in the synthesis of HPF-1. (b) Microspheres formed by the HPF-1 as seen from the FE-SEM. (c) Shows the ^{13}C-MASNMR (400MHz) of HPF-1, the peaks corresponding to aromatic backbone and triazine groups can be observed. Few of the peaks in the aliphatic region corresponds to the occluded THF and Dioxan molecule in the polymer labelled as 's'.

The Field Emission-SEM image indicated the sample to be highly homogeneous microspheres (Figure 1b & S2). Thermogravimetric analysis revealed exceptional thermal stability of up to 380ºC (Figure S3). We attribute the stability of HPF-1 to the strong C-C bond formed between the monomers, characteristic of Bakelite.[48,57] Solid state NMR indicated the presence of Bakelite type couplings (Figure 1c), along with some unsubstituted sites on the resorcinol rings and very few terminal aldehyde groups, which agreed well with the stretching frequencies observed in the Infrared spectra (Figure S4).

Results and discussion

The porosity of HPF-1 was established using N_2 adsorption carried out at 77K (Figure 2a). HPF-1 has a Brunauer–Emmett–Teller (BET) surface area of 576 $m^2 g^{-1}$ and a Langmuir surface area of 777 $m^2 g^{-1}$. A Density functional theory based model fitted to the adsorption branch of the 77K N_2 isotherm showed majority of the pores being 5.5Å in size (Inset of Figure 2a). Different preparation batches were screened and they gave the same uptake indicating HPF-1 forming as a pure phase with good reproducibility. At 195K, the material showed a CO_2 uptake of 9.35 mmol g^{-1}, which represents the saturation CO_2 uptake capacity of the material (Figure 2b). The material showed a moderate CO_2 uptake of 2.8 mmol g^{-1} at 303K, which is the one of the highest uptake reported for a porous polymer under ambient conditions (Table S1, selected porous polymers have been compared in this table). Encouraged by seeing very low uptake of N_2 at room temperature, we carried out CO_2 and N_2 adsorptions at different temperatures.

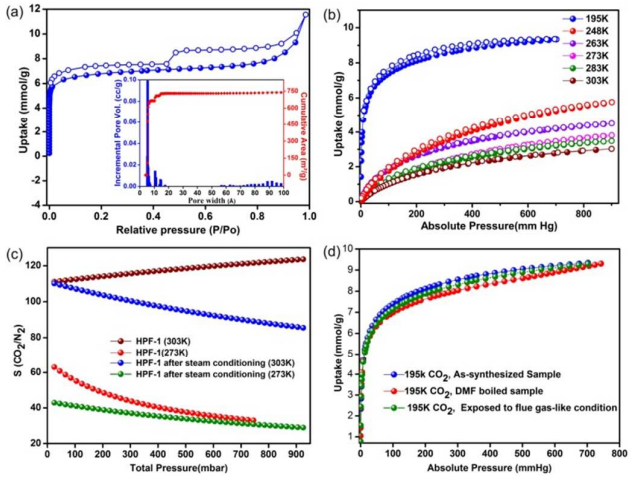

Figure 2. (a) Shows the 77K N_2 adsorption isotherm of HPF-1. Inset shows the pore size distribution with high concentration of ultra-micropore (5.5Å) and a hierarchy of pores in the mesoporous regime but in extremely small relative concentrations. (b) Variable temperature CO_2 isotherm with a saturation uptake of ~9.5 mmol g^{-1} at 195K and a 2.8 mmol g^{-1} at 303K, 1bar. (c) The IAST based CO_2/N_2 selectivity, it drops down in the presence of humidity, however is still quite high (90) at 303K. (d) Comparison of the 195K saturation CO_2 isotherms of acid (conc.HNO_3+ SO_3(g)+ boiling water) and solvent (DMF, 150°C) treated HPF-1.

Ideal Adsorption Solution Theory (IAST) model was used to calculate the selectivity for CO_2 over N_2 for 85%N_2:15%CO_2 composition. It turns out that HPF-1 has a selectivity of 120:1 for CO_2 at 303K and 1 bar pressure (Figure 2c). This is quite high (Table S1) and can be attributed to the inherent molecular sieving effect of the ultra-micropores. Interestingly, the selectivity increases with increasing temperature, this is quite rare in porous polymers.[20] This arises due to the CO_2 capacity dropping down much gradually compared to the N_2 with increasing temperatures. This could be due to the stronger interaction of weakly acidic CO_2 with the triazine lined framework compared to N_2. Such interactions would definitely be exaggerated in small micropores as those present in the polymer.

Chemical stability towards harsh conditions such as acidic vapors, hydrolytic stability under steam and boiling water for such porous materials could make them potential candidates for a variety of application including flue gas capture. A typical gas-fired flue gas consists of the composition 7.4-7.7% CO_2, 14.6% H_2O, ~ 4.45% O_2, 200-300 ppm CO, 60-70 ppm NOx, and 73-74% N_2.[58] If a material stable to these harsh conditions can show good low-pressure CO_2 uptake and recyclability, they could make apt candidate for vacuum swing CO_2 separation applications.[59,60] With this aim, we subjected HPF-1 to a steady stream of acidic vapors generated by heating a solution containing sulfur trioxide, SO_3(g) (generated from chlorosulfonic acid) + conc.HNO_3 + H_2O for about 48hrs. Considering the organic nature of HPF-1, in a separate test, we boiled it in water, DMF, water/DMF, DMF/DMSO, n-butanol and toluene. All the above harsh treatments did not result in any product decomposition or any drop in the porosity of the material, as evidenced from their saturation CO_2 uptakes at 195K (Figure 2d). Demonstration of stability under such harsh chemical environments have been identified as crucial and few studies on porous organic frameworks and metal organic frameworks have been reported recently.[18,61]

To understand the nature of the pore surface in this polymer, as it is functionalized with polar phenolic groups, we carried out vapor sorption studies using water and toluene as probes. It could be seen that the water sorption isotherm had a type III behavior indicating weak adsorbate-adsorbent interactions (Figure 3a). The heat of adsorption (HOA) calculated using a virial analysis showed a value of 43 kJ mol^{-1} at zero-loading (Figure 3b), which is lower than what was reported for a hydrophobic material and is just below the heat of vaporization of water.[54] The toluene adsorption however shows a type I behavior. This is reflected in the HOA for toluene with a value of 35 kJ mol^{-1} at zero-loading, which builds up to a value as high as 62 kJ mol^{-1} at 2.2 mmol g^{-1} loading. This could be due to strong adsorbate-adsorbate interactions which can be expected for toluene molecules trapped in confined pores. Thus, HPF-1 clearly has stronger interactions with toluene than water. A contact angle measurement on a sample that was prepared by spreading the as-synthesized HPF-1 powder on a glass substrate showed a contact angle of 153° for water(Figure 3c), which confirms its highly hydrophobic surface. Some of the super-hydrophobic polymers touted for their hydrophobicity have this value at 164°.[62] In spite of such high contact angle, there is not much selectivity towards toluene in the sorption measurements suggesting that the interior of the material, comprising the pores, are not as hydrophobic as the surface.

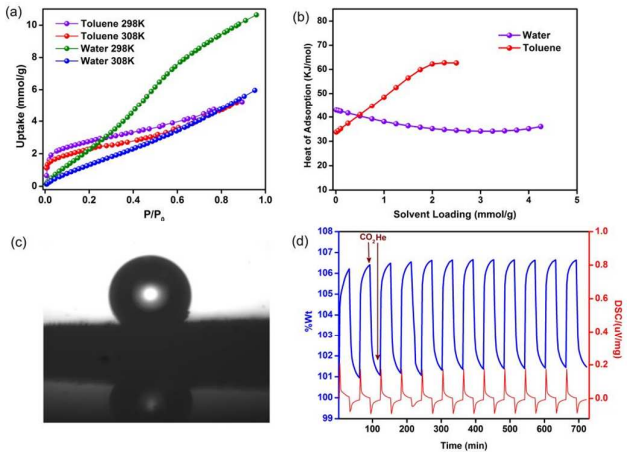

Figure 3. (a) Vapor sorption isotherms of HPF-1 carried out at different temperatures. The toluene shows a type-I behavior while water shows hardly any adhesion, as indicated by a near-linear isotherm. (b) The HOA is consistent with the shapes of the isotherms indicating water is interacting very weak with a zero-loading HOA of 40 kJ mol^{-1} which is near its vaporization point. (c) Contact angle measurement of HPF-1 showing a highly hydrophobic surface (153º). (d) TGA cycling experiments indicating a facile removal of adsorbed CO_2 by a He purge.

A zero-loading heat of adsorption for CO_2 in the range of 25-35 kJ mol^{-1} is indicative of a facile CO_2 recovery.[63] In HPF-1, the HOA of CO_2, estimated from a virial/DFT model, had a moderate value of 26 kJ mol^{-1}, implying the possibility of a facile CO_2 regeneration. We have demonstrated this experimentally through a TGA cycling experiment. A near 100% recovery of adsorbed CO_2 by a He sweep at 303K was obtained on the TGA and fifteen such adsorption/desorption cycles have been carried out without any loss in capacity (Figure 3d). From the water sorption studies it is clear that HPF-1 has relatively weak interactions with water, but the uptake of water is still appreciable. This makes it imperative to demonstrate the ability of the material to adsorb CO_2 even after being exposed to sufficient water or in other words the selectivity of CO_2 over water. For this purpose we have carried out a steam conditioning study wherein other porous materials, with comparable CO_2 uptakes, carbon molecular sieves, ZnAtzOx,[64] zeolite 4A and the title material were activated and then exposed to a flow of humid N_2 (100 ml min-1 over a 75% RH obtained from a saturated NaCl solution maintained at 60ºC) for a period of 24hrs. This wet material was tested for CO_2 adsorption without any further activation. As can be seen from Figure 4, microporous carbon molecular sieve (3kType-172CMS) loses 39% of its CO_2 capacity and ZnAtzOx loses 55%, zeolite 4A loses 83%, while HPF-1 loses 20% of its CO_2 capacity. Even a hydrophobic standard, silica-alumina (P/N 004/16821/00), loses 40% of its CO_2 capacity (See section 9 of supporting info.). As can be seen from Figure 2c, HPF-1's CO_2/N_2 selectivity drops down in the presence of humidity, however even for this steam conditioned phase, the selectivity is still quite high (90) at 303K. And this capacity and selectivity were intact even after 48hrs of steam conditioning.

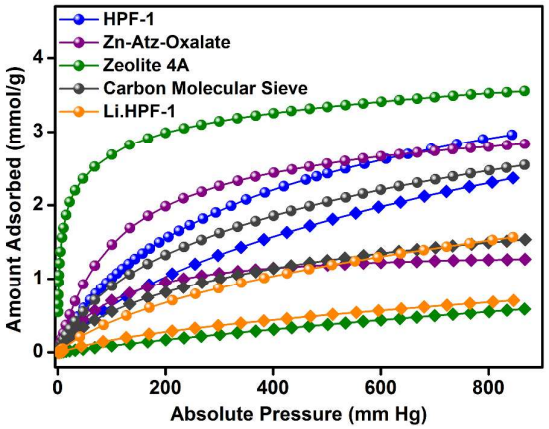

Figure 4. Comparison of the effect of humidity on the CO_2 adsorption behavior of selected porous materials with varying hydrophobic-hydrophilic character and similar CO_2 uptakes. All isotherms were carried out at 303K. *Important: After the steam conditioning the material was not subjected to any activation.* Note: spheres represent activated phase; squares represent steam conditioned phase.

To quantify the CO_2 adsorption of HPF-1 from a dynamic humid CO_2 stream, in a separate and simple experiment, we activated (evacuated at 160ºC for 12hrs. under 10^{-4}Torr) about 1 gm of the sample and then exposed it to a flow of humid CO_2 (100 ml min-1 over a 75% RH obtained from a saturated NaCl solution maintained at 60ºC) for 24hrs. This sample was then cut off from the CO_2 stream and was exposed to ambient conditions to release any CO_2 filling the vessel. The adsorbed CO_2 was desorbed by heating the sample at 60ºC and the evolved CO_2 was captured on to a pre-treated solution of CaO (see supporting information). Brisk bubbling was observed followed by the occurrence of white crystalline precipitate of $CaCO_3$, which was extracted by filtration and dried with a acetone wash. Following this, a mass balance was carried out, which indicated the formation of 0.266g of $CaCO_3$ from 1g of HPF-1.$(CO_2)_x$, which translates to 2.66 mmol g^{-1} of CO_2 per gram of HPF-1. This is 5% less than the capacity obtained from single component CO_2 isotherm. The humidity to which the sample has been exposed during this experiment is much higher than the maximal humidity (15%) expected in a flue gas. Furthermore, the $CaCO_3$ formed was characterized to be anhydrous $CaCO_3$ (ICSD: 18165) using PXRD and the TGA indicated a weight loss agreeing extremely well with what was expected for a 2.66 mmol of CO_2 per gram of HPF-1 (Figure S16).

During our investigation on porous hydrophobic materials, we made an interesting observation that a MOF made up of alternating fluorine and amine lining did not show any CO_2 uptake.[65] Thus, it could be possible that just the presence of hydrophobic sites proximal to a strongly CO_2 interacting site is

not sufficient to obtain good CO_2-framework interactions over water. Or in other words, there has to be an optimal hydrophobic-hydrophilic balance provided by the adjacently positioned functional groups giving rise to adsorption pockets that could favor a less polar CO_2 over water. Here the phenol groups could be providing such hydrophobic-polar environments, as they are known to act as partitioning agents due to their ability to tune its hydrophilic-hydrophobic character depending on the type of substituent on the ring or the environment it is suspended in.[66] To demonstrate the role of the phenolic groups in contributing to the materials hydrophobicity, in another experiment, we loaded the material with ~17% of Li (quantified from Microwave Plasma Atomic Emission Spectrometry) and this lithiated sample was subjected to the same steam conditioning treatment. The CO_2 adsorption studies on this humidified lithiated sample showed a drastic 56% drop in CO_2 capacity (Figure 4). A video has been presented in the supporting information to demonstrate the complete loss of surface hydrophobicity with this ~17% Li loading, clearly expressing the critical role of phenol groups in providing hydrophobic texture to the material.

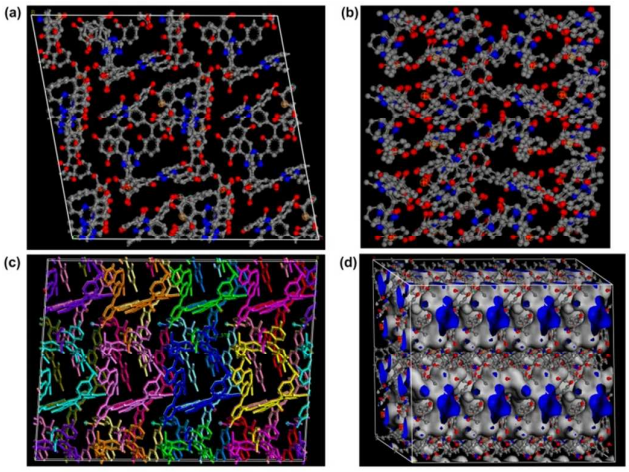

Figure 5. Three dimensional packing of the lowest energy configuration, α- phase, of HPF-1 formed using a random polymerization of monomeric units with terephthaldehyde (DFT-TB minimized). A view along (a) the C-axis showing the small cavities (4 x 8.0 Å), hydrogens have been removed for clarity; (b) the B-axis showing the ultra-micropores (7.5 x 7.0 Å, not factoring the van der Wall radii); (c) Representation differentiating single oligomer of specific site symmetry via different color coding. (d) The Connolly representation of HPF-1 showing the presence of highly corrugated channels running along all three-directions (Blue -opening to the pores).

In recent times, a simulation based approach has been shown to bring significant structural insights on porous polymers.[47,55,56] Experimental structure determination is almost impossible owing to the lack of solubility in these highly cross-linked polymers preventing the use of techniques such as gel permeation chromatography or routine solution NMR. To obtain a probable structure of HPF-1, we created a small oligomer by combining the monomers in 2:3 ratio and minimized its structure using DFT methods with Material Studio. Then we carried out a random polymerization with it to obtain larger oligomer (polymer). The polymer thus generated could take different configurations depending on the slight differences in the geometry of the initial energy minimized smaller oligomer. However, the geometric constraints in terms of acceptable bond lengths, angles and van der Waal distances applied during these operations avoided the generation of too many metastable structures with shallow local minima. Three low energy polymer configurations were chosen based on the final energy (alpha-, beta and gamma, Figure S16). These were then minimized again using tight binding DFT methods (DFT-TB). Following this, an amorphous cell was created independently for the alpha, beta and gamma phases. Again, a DFT tight binding calculation was done to optimize the geometry, lattice parameters and the energy. This yielded a structure with a triclinic cell: P 1; a=37.8895 Å b=35.1144 Å c=23.5303 Å α=89.768(2)° β=91.638(4)° γ=100.648(4)° (Figure 5). During the entire process complete rotational and torsional freedom was maintained. We remark that only when the initial oligomer was properly geometry optimized, could the larger oligomer be formed with acceptable bonds and favorable van der Waal requirements. The lowest energy polymer configuration, alpha, had relative energies two and three times lower than the beta and gamma respectively (Figures 5 and S18). The structure of the alpha phase had highly corrugated ultra-micropores, which are lined by the phenol groups from the resorcinol unit and the nitrogens of the triazine groups protrude along the walls making them accessible. A Connolly representation shows the presence of three-dimensional access via small ultra-microporous openings (Figure 5d). The surface area calculations done using Material Studio yielded a theoretical surface area of 570 $m^2 g^{-1}$ (Exptl. BET, 77K N_2: 576 $m^2 g^{-1}$) and pore volume of 0.24 $cm^3 g^{-1}$ (Exptl., 77K N_2: 0.27 $cm^3 g^{-1}$). We simulated the pure-component (0-1bar) isotherms at 303K for both CO_2 and N_2 for all the three configurations using a Monte-Carlo method (Accelrys).[64] The simulated isotherm matched exceptionally well with the experimental one (Figure 6a), but only for the alpha form. From the simulations, the average heat of adsorption was estimated at 30 kJ mol^{-1} which is very close to the experimentally determined 26 kJ mol^{-1} (In set of Figure 6a).

The complex pore structure of HPF-1 comprising of extremely corrugated channels could pose possible diffusion limitations to the movement of CO_2 molecules across the polymer. To address this, the diffusion of CO_2 within the hydrophobic-polar channels of the HPF-1 was measured using rate of adsorption studies. The equilibration kinetics associated with 10 different pressure points were extracted and the data was fitted to a spherical pore model (Figure S19).[67]

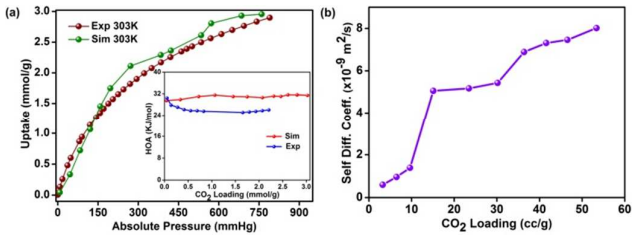

Figure 6. Shows (a) Comparison of the CO_2 isotherm simulated using α- phase and the experimental isotherm at 303K. Inset shows the comparison of the HOA plots. (b) The Self-diffusion coefficient for CO_2 in HPF-1 fitted using a spherical pore model.

A CO_2 self-diffusivity coefficient of 10^{-9} m^2 sec^{-1} was calculated, (Figure 6b) which is higher than the value obtained for zeolites and is comparable to some of the MOFs.[68-70] In fact, this diffusivity values are similar to those obtained for htfp, a highly hydrophobic MOF, built from ligands rich in aromatic groups.[68] Also, the CO_2 diffusion in HPF-1 appears considerably facile compared to a fluorine lined ultra-microporous MOF.[71] This could be due to the relatively weaker framework-CO_2 interactions in HPF-1. The CO_2 self-diffusivities used in these comparisons are for materials that are being used in industrial CO_2 capture and the ones that have been identified as potential candidates. However, there is marked difference in the pathways that CO_2 would be travelling through, this difference arises from the pore sizes and also from the structure of the pore walls.[4] Given this, the MOFs and porous organic polymers with larger pores and with soft or flexible pore walls are always expected to have an advantage over zeolites with narrow windows and rigid pore walls. The jumps found in the diffusivity values with increasing CO_2 loadings (Figure 6b) could be due to the corrugated pores making the structure digress from the spherical model. Yet, other models (linear or slab) did not fit well. To the best of our knowledge, till date there are no reports of CO_2 kinetics in porous polymers.

Conclusions

Here, we have synthesized a porous polymer by employing a tri-resorcinol with a triazine core as the building unit. The emphasis of the material includes its ability to selectively capture CO_2 over N_2, and its exceptional stability to harsh conditions (NOx, SOx, Steam) that mimic flue gas environments. Such stability from a porous material is highly desirable and we attribute it to the lack of hydrolyzable groups and the polymer backbone being built up from C-C bonds. When the adsorption was carried out using a humid CO_2 stream the material loses only about 5% of its capacity, still having a selectivity of 90:1. Converting 17% of the phenol groups into -OLi results in complete loss of the surface hydrophobicity exemplifying the role of phenolic groups in providing hydrophobicity. To obtain structural insights that could explain the hydrophobic-hydrophilic character of the material, we have proposed a structure based on amorphous cell simulation. HPF-1 has corrugated ultra-microporous channels copiously lined by phenol groups and basic triazine units which agrees extremely well with our expectations of the pore surface based on solvent sorption studies and preferential CO_2 sorption. The 303K CO_2 adsorption isotherms and the associated HOA profiles simulated based on this structure seem to match well with the experimentally observed ones, which adds to the confidence of the proposed structure. In fact, HPF-1 brings out a phenol-triazine-aldehyde based chemistry which enables us to develop porous polymers with a fine balance between hydrophobicity and polar character. The catalyst free and easily up scalable synthesis and cheap ingredients make this class of materials an attractive target.

Acknowledgements

We gratefully acknowledged IISER Pune and MHRD, Govt. of India for financial support. S. Nandi Thanks DST, CII, SERB and Enovex for financial support through Prime Minister Fellowship.

Notes and references

1 H.-C. Joe-Zhou, S. Kitagawa, *Chem. Soc. Rev.,* 2014, **43**, 5415.
2 J. M. Huck, L. -C. Lin, A. H. Berger, M. N. Shahrak, R. L. Martin, A. S. Bhown, M. Haranczyk, K. Reuter, B. Smit, *Energy Environ. Sci.,* 2014, **7**, 4132.
3 M. E. Boot-Handford, J. C. Abanades, E. J. Anthony, M. J. Blunt, S. Brandani, N. M. Dowell, J. R. Fernández, M.-C. Ferrari, R. Gross, J. P. Hallett, R. S. Haszeldine, P. Heptonstall, A. Lyngfelt, Z. Makuch, E. Mangano, R. T. J. Porter, M. Pourkashanian, G. T. Rochelle, N. Shah, J. G. Yaoa, P. S. Fennell, *Energy Environ. Sci.,* 2014, **7**, 130.
4 J. Liu, P. K. Thallapally, B. P. McGrail, D. R. Brown, J. Liu, *Chem. Soc. Rev.,* 2012, **41**, 2308.
5 K. Sumida, D. L. Rogow, J. A. Mason, T. M. McDonald, E. D. Bloch, Z. R. Herm, T. -H. Bae, J. R. Long, *Chem. Rev.,* 2012, **112**, 724.
6 M. J. Bojdys, J. Jeromenok, A. Thomas, M. Antonietti, *Adv. Mater.* 2010, **22**, 2202.
7 A. I. Cooper, *CrystEngComm*, 2013, **15**, 1483.
8 Z. Zhang, Z. -Z. Yao, S. Xiang, B. Chen, *Energy Environ. Sci.,* 2014, **7**, 2868.
9 P. Nugent, Y. Belmabkhout, S. D. Burd, A. J. Cairns, R. Luebke, K. Forrest, T. Pham, S. Ma, B. Space, L. Wojtas, M. Eddaoudi, M. J. Zaworotko, *Nature* 2013, **495**, 80.
10 Z. Zhang, Y. Zhao, Q. Gong, Z. Lib, J. Li, *Chem. Commun.,* 2013, **49**, 653.
11 Q. Wang, J. Luo, Z. Zhong, A. Borgna, *Energy Environ. Sci.*, 2011, **4**, 42.
12 T. C. Drage, C. E. Snape, L. A. Stevens, J. Wood, J. Wang, A. I. Cooper, R. Dawson, X. Guo, C. Satterley, R. Irons, *J. Mater. Chem.,* 2012, **22**, 2815.
13 J. Wang, L. Huang, R. Yang, Z. Zhang, J. Wu, Y. Gao, Q. Wang, D. O'Hare, Z. Zhong, *Energy Environ. Sci*., 2014, **7**, 3478.
14 C. Mottillo, T. Friscic, *Angew. Chem., Int. Ed. Engl.,* 2014, **53**, 7471.
15 D. Feng, K. Wang, J. Su, T.-F. Liu, J. Park, Z. Wei, M. Bosch, A. Yakovenko, X. Zou, H.-C. Zhou, *Angew. Chem. Int. Ed. Engl*., 2015, **54**, 149.
16 S. B. Kalidindi, S. Nayak, M. E. Briggs, S. Jansat, A. P. Katsoulidis, G. J. Miller, J. E. Warren, D. Antypov. F. Cor, B.

Slater, M. R. Prestly, C. M. Gastaldo, M. J. Rosseinsky, *Angew. Chem., Int. Ed. Engl.,* 2015, **54**, 221.
17 T. A. Makal, X. Wang, H.-C. Zhou, *Cryst. Growth Des.,* 2013, **13**, 4760.
18 Q. Liu, L. Ning, S. Zheng, M. Tao, Y. Shi, Y. He, *Sci. Rep.,* 2013, **3**, 2916.
19 Y. Liu, Z. U. Wang, H.-C. Zhou, *Greenhouse Gas:Sci Technol.*, 2012, **2**, 239.
20 H. A. Patel, S. H. Je, J. Park, D. P. Chen, Y. Jung, C. T. Yavuz, A. Coskun, *Nat. Commun.* 2013, **4**, 1357.
21 H. A. Patel, F. Karadas, A. Canlier, J. Park, E. Deniz, Y. Jung, M. Atilhan, C. T. Yavuz, *J. Mater. Chem.*, 2012, **22**, 8431.
22 X. Zhu, S. M. Mahurin, S.-H. An, C. -L. Do-Thanh, C. Tian, Y. Li, L. W. Gill, E. W. Hagaman, Z. Bian, J. -H. Zhou, J. Hu, H. Liu, S. Da, *Chem. Commun.,* 2014, **50**,7933-7936.
23 H. M. El-Kaderi, J. R. Hunt, J. L. Mendoza-Cortés, A. P. Côté, R. E. Taylor, M. O'Keeffe, O. M. Yaghi, *science,* 2007, **316**, 268.
24 Y. Luo, B. Li, W. Wang, K. Wu, B. Tan, *Adv. Mater.*, 2012, **24**, 5703.
25 P. Arab, M. G. Rabbani, A. K. Sekizkardes, T. İslamoğlu, H. M. El-Kaderi, *Chem. Mater.*, 2014, **26**, 1385.
26 J. Lua, J. Zhang, *J. Mater. Chem. A,* 2014, **2**, 13831.
27 T. Ben, H. Ren, S. Ma, D. Cao, J. Lan, X. Jing, W. Wang, J. Xu, F. Deng, J. M. Simmons, S. Qiu, G. Zhu, *Angew. Chem., Int. Ed. Engl.*, 2009, **48**, 9457.
28 Y. Li, T. Ben, B. Zhang, Y. Fu, S. Qiu, *Sci. Rep.*, 2013, **3**, 2420.
29 A. Thomas, *Angew. Chem., Int. Ed. Engl.*, 2010, **49**, 8328.
30 A. I. Cooper, *Adv. Mater.,* 2009, **21**, 1291.
31 D. Q. Yuan, W. G. Lu, D. Zhao, H. C. Zhou, *Adv. Mater*., 2011, **23**, 3723.
32 G. Qi, Y. Wang, L. Estevez, X. Duan, N. Anako, A.-H. A. Park, W. Li, C. W. Jones, E. P. Giannelis, *Energy Environ. Sci.,* 2011, **4**, 444.
33 M. Rose, W. Bohlmann, M. Sabo, S. Kaskel, *Chem. Commun*., 2008, 2462.
34 C. F. Martín, E. Stöckel, R. Clowes, D. J. Adams, A. I. Cooper, J. J. Pis, F. Rubiera, C. Pevida, *J. Mater. Chem.*, 2011, **21**, 5475.
35 A. Bhunia, I. Boldog, A. Möller, C. Janiak, *J. Mater. Chem. A*, 2013, **1**, 14990.
36 A. Bhunia, V. Vasylyeva, C. Janiak, *Chem. Commun.*, 2013, **49**, 3961.
37 M. G. Schwab, B. Fassbender, H. W. Spiess, A. Thomas, X. Feng, K. Müllen, *J. Am. Chem. Soc.*, 2009, **131**, 7216.
38 N. Du, H. B. Park, G. P. Robertson, M. M. Dal-Cin, T. Visser, L. Scoles, M. D. Guiver, *Nat. Mater*., 2011, **10**, 372.
39 J.-X. Jiang, F. Su, A. Trewin, C. D. Wood, N. L. Campbell, H. Niu, C. Dickinson, A. Y. Ganin, M. J. Rosseinsky, Y. Z. Khimyak, A. I. Cooper, *Angew. Chem., Int. Ed. Engl.*, 2007, **46**, 8574.
40 R. Dawson, E. Stöckel, J. R. Holst, D. J. Adams, A. I. Cooper, *Energy Environ. Sci.,* 2011, **4**, 4239.
41 S. Sung, M. P. Suh, *J. Mater. Chem. A*, 2014, **2**, 13245.
42 H. He, W. Li, M. Zhong, D. Konkolewicz, D. Wu, K. Yaccato, T. Rappold, G. Sugar, N. E. David, K. Matyjaszewski, *Energy Environ. Sci.,* 2013, **6**, 488.
43 G. P. Hao, W-. C. Li, D. Qian, G-. H. Wang, W-. P. Zhang, T. Zhang, A-. Q. Wang, F. Schüth, H-. J. Bongard, A-. H. Lu, *J. Am. Chem. Soc.*, 2011, **133**, 11378.
44 J. Yu, P. B. Balbuena, *J. Phys. Chem. C,* 2013, **117**, 3383.
45 P. Markewitz, W. Kuckshinrichs, W. Leitner, J. Linssen, P. Zapp, R. Bongartz, A. Schreibera, T. E. Muller, *Energy Environ. Sci.,* 2012, **5**, 7281.
46 J. -H. Zhu, Q. Chen, Z. -Y. Sui, L. Pan, J. Yu, B.-H. Han, *J. Mater. Chem. A,* 2014, **2**, 16181.
47 B. Li, R. Gong, W. Wang, X. Huang, W. Zhang, H. Li, C. Hu, B. Tan, *Macromolecules*, 2011, **44**, 2410.
48 A. P. Katsoulidis, M. G. Kanatzidis, *Chem. Mater.*, 2011, **23**, 1818.
49 A. K. Sekizkardes, S. Altarawneh, Z. Kahveci, T. İslamoğlu, H. M. El-Kaderi, *Macromolecules*, 2014, **47**, 8328.
50 M. Saleh, S. B. Baek, H. M. Lee, K. S. Kim, *J. Phys. Chem. C*, 2015, **119**, 5395.
51 G. K. H. Shimizu, R. Vaidhyanathan, J. M. Taylor, *Chem. Soc. Rev.*, 2009, **38**, 1430 .
52 F. Sua, C. Lu, *Energy Environ. Sci.*, 2012, **5**, 9021.
53 Z. Zhang, W. Zhang, X. Chen, Q. Xia, Z. Li, *Sep. Sci. Technol.*, 2010, **45**, 710.
54 J. M. Taylor, R. Vaidhyanathan, S. S. Iremonger, G. K. H. Shimizu, *J. Am. Chem. Soc.*, 2012, **134**, 14338.
55 C. Reece, D. J. Willock, A. Trewin, *Phys. Chem. Chem. Phys.,* 2015, **17**, 817.
56 J.-X. Jiang, F. Su, A. Trewin, C. D. Wood, H. Niu, J. T. A. Jones, Y. Z. Khimyak, A. I. Cooper, *J. Am. Chem. Soc.*, 2008, **130**, 7710.
57 A. P. Katsoulidis, J. He, M. G. Kanatzidis, *Chem. Mater.*, 2012, **24**, 1937;
58 X. Xu, C. Song, R. Wincek, J. M. Andresen, B. G. Miller, A. W. Scaroni, *Fuel Chemistry Division,* 2003, **48**, 162.
59 S. Xiang, Y. He, Z. Zhang, H. Wu, W. Zhou, R. Krishna, B. Chen, *Nat. Commun.,* 2012, **3**, 954.
60 J. A. Mason, K. Sumida, Z. R. Herm, R. Krishna, J. R. Long, *Energy Environ. Sci.,* 2011, **4**, 3030.
61 R. T. Woodward, L. A. Stevens, R. Dawson, M. Vijayaraghavan, T. Hasell, I. P. Silverwood, A. V. Ewing, T. Ratvijitvech, J. D. Exley, S. Y. Chong, F. Blanc, D. J. Adams, S. G. Kazarian, C. E. Snape, C. T. Drage, A. I. Cooper, *J. Am. Chem. Soc.,* 2014, **136**, 9028.
62 K.P. Rao, M. Higuchi, K. Sumida, S. Furukawa, J. Duan, S. Kitagawa, *Angew. Chem., Int. Ed. Engl.,* 2014, **126**, 8364.
63 J. M. Simmons, H. Wu, W. Zhou, T. Yildirim, *Energy Environ. Sci.*, 2011, **4**, 2177.
64 R. Vaidhyanathan, S. S. Iremonger, G. K. H. Shimizu, P. G. Boyd, S. Alavi, T. K. Woo, *Science*, 2010, **330**, 650.
65 C. Y. Su, A. M. Goforth, M. D. Smith, P. J. Pellechia, H. C. zur Loye, *J. Am. Chem. Soc.*, 2004, **126**, 3576
66 S. Katsuta, K. Nakamura, Y. Kudo, Y. Takeda, H. Kato, *J. Chem. Eng. Data,* 2011, **56** , 4083.
67 K. Malek, M. -O. Coppens, *J. Chem. Phys.*, 2003, **119**, 2801.
68 L. Zhang, G. Wu, J. Jiang, *J. Phys. Chem. C,* 2014, **118**, 8788.
69 F. Salles, H. Jobic, A. Ghoufi, P. L. Llewellyn, C. Serre, S. Bourrelly, G. Frey, G. Maurin, *Angew. Chem., Int. Ed. Engl.,* 2009, **48**, 8335 .
70 J. A. C. Silva, K. Schumann, A. E. Rodrigues, *Microporous Mesoporous Mater.,* 2012, **158**, 219 .
71 K. A. Forrest, T. Pham, A. Hogan, K. McLaughlin, B. Tudor, P. Nugent, S. D. Burd, A. Mullen, C. R. Cioce, L. Wojtas, M. J. Zaworotko, B. Space, *J. Phys. Chem. C*, 2013, **117**, 17687.